Temperature and Molecular Weight Dependence of the Viscometric Properties of Main-Chain Liquid Crystal Polymers in Nematic Solvents

Fu-Lung Chen and A. M. Jamieson*

Department of Macromolecular Science, Case Western Reserve University, Cleveland, Ohio 44106

Received February 28, 1994; Revised Manuscript Received June 6, 1994®

ABSTRACT: The twist and bend viscosities of dilute nematic solutions in 4′-(pentyloxy)-4-cyanobiphenyl (5OCB) and in 4′-pentyl-4-cyanobiphenyl (5CB) of the main-chain liquid crystal polymers, TPB10 and TPB13, which have a mesogenic group, 1-(4-hydroxy-4′-biphenyl)-2-(4-hydroxyphenyl)butane, separated, respectively, by flexible decamethylene and tridecamethylene spacers, were determined via dynamic light scattering analysis. A theoretical expression for the increment of twist viscosity, γ_1, derived by Brochard can be applied to interpret the experimental results in terms of changes in the mean square end-to-end distances parallel ($R_\parallel^2$) and perpendicular ($R_\perp^2$) to the nematic director. We find that the hydrodynamic behavior of TPB10 oligomers moves closer to that predicted for a rigid rod as the temperature decreases. By modeling the oligomers as a mixture of configurational isomers, the hairpin probability per repeat unit and the associated activation energy can be found. The latter is approximately twice the energy barrier of a trans to gauche transformation. As the molecular weight is increased from oligomers to polymers a decrease in the exponent characterizing the contour length dependence of the intrinsic twist and bend viscosities, $[\gamma_1]$ and $[\eta_{bend}]$, is found, emblematic of a crossover from rigid rod to biased random walk behavior. The effect of absolute temperature on the viscometric properties of TPB13 polymer (GPC determined M_w = 79100 g/mol) was studied by comparing the viscosity in high and low temperature nematic solvents at equal order parameters, viz. TPB13/5CB at T = 27.3 °C and TPB13/5OCB at T = 62.0 °C. A large increase in $[\gamma_1]$ but negligible change in $[\eta_{bend}]$ was found on decreasing temperature.

Introduction

Main-chain nematic liquid crystal polymers (LCP) have very different configurational statistics and viscoelastic behavior in the nematic state versus the isotropic state, because the nematic field has a strong effect on the internal molecular degrees of freedom. Thus, when a LCP is dissolved in a nematic solvent (NS), the LCP chain adopts an anistropic shape which is determined by the competition between the three-dimensional entropic expansion and the tendency of the mesogenic groups to be aligned with the nematic field. The anisotropic radii of gyration, $R_{g,\parallel}$ and $R_{g,\perp}$, of the LCP chains in nematic media have been determined by small angle X-ray scattering[1] and small-angle neutron scattering (SANS).[2] Here, $\parallel$ and $\perp$ refer to measurements parallel and perpendicular, respectively to the nematic director, i.e. to a unit vector oriented along the average nematic axis. Recently, there has been interest in investigating the viscoelastic properties of nematic solutions containing a LCP dissolved in a nematic solvent, which are expected to be a sensitive function of the LCP molecular architecture.[3-15] The elastic constants and viscosity coefficients which characterize the splay, twist, and bend distortions of the nematic solution can be determined via the associated Freedericksz transition characteristics under magnetic or electric fields,[16,17] and by static and dynamic light scattering measurements,[3,18-20] in each case performed on nematic monodomains. A theoretical model developed by Brochard[21] provides expressions which express certain viscosity increments as a function of the mean square end-to-end distances $R_\parallel^2$ and $R_\perp^2$.

In a previous study,[22] we determined the molecular weight dependence of the intrinsic twist viscosity of a main-chain LCP designated TPB10, which has a mesogenic group, 1-(4-hydroxy-4′-biphenyl)-2-(4-hydroxyphenyl)butane, separated by flexible decamethylene spacers. Our experiments were performed on monodisperse TPB10 oligomers and TPB10 polymers of narrow polydispersity, and deduced, using arguments based on the Brochard model[21], that the oligomer hydrodynamic behavior is close to that of a free-draining rigid rod, while the polymer chains behave approximately as free-draining biased random coils. In the same study, by modeling the TPB10 oligomers as mixtures of straight and bent configurational isomers, we could obtain an estimate of the probability of a hairpin turn from the intrinsic twist viscosity data.[22] It is also pertinent to note that the length of the flexible spacer, x, of TPBx influences the viscometric behavior. In particular, we found[15] that the splay viscosity increments for chains with even spacers were larger than those with odd spacers, suggesting that the former had a more extended chain configuration along the director. In addition to the spacer length, we know that there are two other major factors, temperature and nematic potential (or order parameter), which influence the LCP configuration and hence the viscometric properties of an LCP dissolved in a nematic solvent. It is of interest to elucidate the intrinsic temperature effect on the aforementioned viscometric properties and chain statistics. Earlier studies[1,4-9] have evaluated the effect of temperature upon the configurational relaxation time, the increment of twist viscosity, and chain configurational anisotropy. However, these experiments generally utilized a single nematic solvent so that, unavoidably, the nematic potential changes as the temperature changes. In this paper, we seek to isolate the intrinsic temperature dependence of the chain configuration and hydrodynamic behavior by characterizing viscometric properties of a main-chain LCP in high- and low-temperature nematic solvents under conditions of comparable nematic order parameter. In addition, we have also studied for the first time the effects of temperature and molecular weight on the bend distortion of main-chain LCP/NS mixtures.

® Abstract published in *Advance ACS Abstracts*, July 15, 1994.

0024-9297/94/2227-4691$04.50/0

Table 1. Molecular Weights, Chain Contour Lengths, and T_{NI} of TPB10 and TPB13

	specimen								
	TPB10 dimer	TPB10 trimer	TPB10 tetramer	TPB10 no. 5	TPB10 no. 6	TPB10 no. 7	TPB10 no. 8	TPB10 no. 9	TPB13
M_c[a] (g/mol)	1054	1510	1966	-	-	-	-	-	-
$M_{W,GPC}$[b] (g/mol)	1670	2420	3070	13330	17300	25080	245820	75440	79100
(M_w/M_n)[b]	1.0	1.0	1.0	1.18	1.21	1.20	1.28	1.34	≈2
$M_{w,a}$[c] (g/mol)	1054	1510	1966	8440	10950	15860	28990	47730	-
L_w[d] (Å)	81.5	115.4	149.3	629.9	816.6	1181.5	2156.6	3548.5	-
T_{NI}[e] (°C)	62.9	77.9	84.9	103.8	105.9	108.2	112.6	114.0	79.0

[a] Calculated molecular weight. [b] Determined by GPC using chloroform as a solvent and polystyrene as a standard.[23] [c] Actual molecular weight obtained by correcting $M_{W,GPC}$ via the ratio between $M_{W,GPC}$ and M_c of oligomers. [d] Chain contour length based on $M_{w,a}$. [e] From the second heating scan.[23]

TPB10

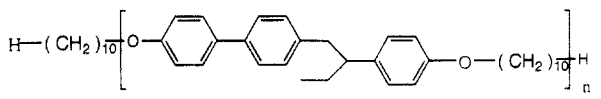

TPB13

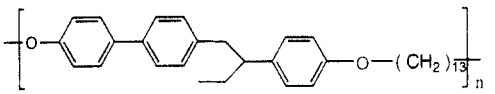

Figure 1. The chemical structures of TPB10 and TPB13: A racemic mixture of each species was utilized in our investigation.

Experimental Section

A. Materials. The main-chain LCPs, TBP10 and TPB13, consist of a mesogenic unit, 1-(4-hydroxy-4′-biphenyl)-2-(4-hydroxyphenyl)butane, separated, respectively, by flexible decamethylene and tridecamethylene spacers. Specimens of these main-chain LCPs were supplied to us by Prof. Virgil Percec, Case Western Reserve University. The chemical structures, molecular weights, chain contour lengths, and nematic-to-isotropic transition temperatures can be found in Figure 1 and Table 1. It is important to recognize that the true molecular weights of the TPBx polymers are expected to be different from the apparent values, measured by GPC relative to polystyrene standards. Experimentally, it was found that[23] the true molecular weights of TPB10 oligomers differ from the GPC values by a nearly constant ratio. We assume that we can use this ratio to obtain more accurate estimates of the true molecular weights for the TPB10 polymers from their GPC values. These corrected molecular weights were further used to calculate the chain contour lengths of TPB10 polymers. 4′-(Pentyloxy)-4-cyanobiphenyl (5OCB, T_{NI} = 67 °C) previously shown[24] to be a nematic solvent for TPB10 and TPB13, was obtained from Aldrich Chemical Co. 4′-Pentyl-4-cyanobiphenyl (5CB, T_{NI} = 34.8 °C), which we find via the contact method[24] to be a solvent for TPB10 oligomers (but not for TPB10 polymers[24]) and TPB13, was purchased from BDH Ltd. All materials were used as received without further purification. Planar (homogeneous) monodomains, in which the average molecular direction is parallel to the glass surfaces, were prepared using rubbed polyimide-coated conductive glass slides graciously supplied to us by Mr. Pat Dunn at Kent State University, Kent, Ohio. Homeotropic monodomains, where the average molecular direction is perpendicular to the glass surfaces, were prepared using conductive glass slides coated with lecithin (Epikuron, Lucas Meyer Inc.). The sample cell thickness was measured by interferometry[25] with an experimental error of 1%. The spacer used in the cell was 25 μm Mylar and the cells were sealed with epoxy (Devcon). Cells were filled with nematic mixtures at temperatures around 65 °C and 40 °C for 5OCB and 5CB solutions, respectively. A Carl Zeiss optical polarizing microscope equipped with a Mettler FP82HT hot stage and a Mettler FP90 central processor was used to evaluate the nematic alignment, based on the fact that, under cross polarizers, homeotropic alignment as well as disclinations in planar alignment appear dark. This method was also used to determine the nematic to isotropic transition temperatures, T_{NI}, of the samples at a heating rate of 0.2 °C/min. Note that all of the TPB10 oligomers except the monomer, and all the polymers, show nematic states whose T_{NI} are reported in Table 1.

B. Dynamic Light Scattering. A detailed description of the methods and analytical procedures for the application of dynamic light scattering to the determination of viscoelastic parameters of nematic liquid crystals can be found elsewhere.[3,18-20] We performed light scattering measurements in the homodyne configuration, using a photon correlation spectrometer equipped with a 6 MW He–Ne linearly polarized laser and a BI-2030AT 264 channel digital correlator. The sample cell was positioned in a refractive index-matching bath containing 4-*tert*-butyltoluene. The sample cell temperature was controlled by a circulating bath to an accuracy of ±0.1 °C. Three VH scattering configurations which have been described in detail previously[3] were utilized in our experiments as follows.

(1) Configuration I (Splay Geometry). The director of a planar monodomain is oriented parallel to the incident polarization. The angles in the lab frame θ_{lab}, i.e. the angle between the transmitted laser beam and the photomultiplier tube, chosen to isolate the pure splay mode are 24.83° for 5OCB mixtures at $\Delta T = T_{NI} - T$ = 5.0 °C and 26.53° for 5CB mixtures at ΔT = 7.5 °C. The decay rate, Γ_1, of the correlation function of light scattered at this geometry can be expressed by[3]

$$\Gamma_1(q) = K_{11}q_\perp^2/\eta_{splay} \tag{1a}$$

$$q_\perp = 2\pi[(n_\parallel - n_\perp \cos\theta)^2 + n_\perp^2 \sin^2\theta]^{0.5}/\lambda_0 \tag{1b}$$

$$\eta_{splay} = \gamma_1 - \alpha_3^2/\eta_b \tag{1c}$$

where K_{11} is the splay elastic constant; λ_0 is the wavelength of incident light in vacuum (632.8 nm); $n_\parallel$ and $n_\perp$ are the extraordinary and ordinary refractive indices of the nematic mixtures; θ is the scattering angle in the nematic mixture and can be calculated by Snell's law, viz. $n_\perp \sin\theta = n_m \sin\theta_{lab}$ where n_m is the refractive index of the matching liquid; α_3 refers to a Leslie viscosity coefficient;[26] γ_1 is the twist viscosity and η_b is a Miesowicz viscosity.[27]

(2) Configuration II (Twist Geometry). The director of a homeotropic monodomain is oriented perpendicular to the incident polarization and parallel to the incident wave vector. The decay rate, Γ_2, can be expressed, in the absence of an electric field parallel to the director, as:[3]

$$\Gamma_2 = (K_{33}q_\parallel^2 + K_{22}q_\perp^2)/\eta_2 \tag{2a-1}$$

and, in the presence of an electric field parallel to the director, as:[28]

$$\Gamma_2 = (K_{33}q_\parallel^2 + K_{22}q_\parallel^2)/\eta_2 + \epsilon_0\Delta\epsilon V^2/(d^2\eta_2) \tag{2a-2}$$

$$\eta_2 = \gamma_1 - [(\eta_a/\alpha_2^2)q_\perp^2/q_\parallel^2 + \eta_c/\alpha_2^2]^{-1} \tag{2b}$$

$$q_\parallel = 2\pi(n_\perp - n\cos\theta)/\lambda_0 \tag{2c}$$

$$q_\perp = (2n\pi\sin\theta)/\lambda_0 \tag{2d}$$

$$n = n_\parallel n_\perp/(n_\perp^2\sin^2\theta + n_\parallel^2\cos^2\theta)^{0.5} \tag{2e}$$

where K_{22} and K_{33} are the twist and bend elastic constants, respectively; λ_0 is the wavelength of incident light in vacuum (632.8 nm); $n_\parallel$ and $n_\perp$ are, respectively, the extraordinary and ordinary refractive indices of the nematic mixtures; θ is the scattering angle in the nematic mixture and can be calculated by

Snell's law, viz. $n \sin\theta = n_m \sin\theta_{lab}$ where n_m is the refractive index of the matching liquid; γ_1 is the twist viscosity; α_2 refers to a Leslie coefficient;[26] η_a and η_c are Miesowicz viscosities;[27] V is the applied voltage across the cell; d is the thickness of the cell; ϵ_0 is the dielectric permittivity in vacuum, and $\Delta\epsilon$ is the dielectric anisotropy of the liquid crystal solution and is defined as $\epsilon_\parallel - \epsilon_\perp$ where $\epsilon_\parallel$ and $\epsilon_\perp$ are the dielectric permittivities parallel and perpendicular, respectively, to the director. From eq 2a-2, it is evident that we can independently measure the pure twist viscosity by performing the electric field-dependent light scattering at one angle if the magnitude of $(\eta_a/\alpha_2^2)q_\perp^2/q_\parallel^2$ is very large. However, since the magnitude of η_a/α_2^2 for our samples is generally very small, the angle at which we can measure the pure twist mode is also very small. It is difficult to perform the light scattering measurements at such small angles due to the flare from the glass surface. We therefore performed electric field-dependent light scattering measurements at several different angles for each sample and determined K_{22} and γ_1 via fits to eq 2a-2.

(2) Configuration III (Bend Geometry). The director of a planar monodomain is oriented perpendicular to both the incident polarization and the incident wave vector. The decay rate, Γ_2, of light scattered in this geometry is[3]

$$\Gamma_2 = (K_{33}q_\parallel^2 + K_{22}q_\perp^2)/\eta_2 \tag{3a}$$

$$\eta_2 = \gamma_1 - [(\eta_a/\alpha_2^2)q_\perp^2/q_\parallel^2 + \eta_c/\alpha_2^2]^{-1} \tag{3b}$$

$$q_\parallel = (2n\pi \sin\theta)/\lambda_0 \tag{3c}$$

$$q_\perp = 2\pi(n_\perp - n\cos\theta)/\lambda_0 \tag{3d}$$

$$n = n_\parallel n_\perp/(n_\parallel^2 \sin^2\theta + n_\perp^2 \cos^2\theta)^{0.5} \tag{3e}$$

Note that from eq 3, we can determine the pure bend mode scattering if $q_\perp = 0$. At this condition, η_2 becomes the bend viscosity, η_{bend}, defined as

$$\eta_{bend} = \gamma_1 - \alpha_2^2/\eta_c \tag{4}$$

The angles in the lab frame θ_{lab} at which we can measure the pure bend mode are 24.83°, 27.51°, and 26.53° for 5OCB mixtures at ΔT = 5.0 and 15.0 °C and 5CB mixtures at ΔT = 7.5 °C, respectively.

C. Freedericksz Transition and Dielectric Permittivity Measurements. Freedericksz transition measurements were performed to measure the splay elastic constant, K_{11}. This technique is described in detail elsewhere.[29] Basically, this method involves monitoring the capacitance of a planar monodomain while an increasing bias voltage (V_b) is applied. A three-terminal arrangement with guard electrodes was used to eliminate edge effects. The frequencies of the bias voltage and probe signal were f_b = 50 Hz and f_s = 6000 Hz, respectively. The K_{11} can be calculated via the following equation:[29]

$$V_{th}^2 = K_{11}\pi^2/(\epsilon_0\Delta\epsilon) \tag{5a}$$

$$\Delta\epsilon = \epsilon_\parallel - \epsilon_\perp \tag{5b}$$

where V_{th} is the threshold voltage, ϵ_0 is the dielectric permittivity in vacuum, and $\Delta\epsilon$ is the dielectric anisotropy. $\epsilon_\perp$ was obtained by measuring the capacitance of a planar monodomain at zero field. $\epsilon_\parallel$ was obtained by measuring the capacitance of a homeotropic monodomain in the presence of a 7 volt bias voltage (3000 Hz) to improve the alignment.

For TPB13/5CB, pure 5CB, TPB13/5OCB, and pure 5OCB, all the above cited experiments were performed to obtain information on all the various viscosities. For TPB10/5OCB and TPB10/5CB, we only determined the decay rates of light scattered by the pure bend mode and of electric field-dependent light scattering in the twist geometry (configuration II).

Results and Discussion

a. Twist Viscosity of TPB10 Oligomers. Figure 2 shows the viscosity function η_2 at various scattering angles in the lab frame, together with the least squares fits to eq 2a-2, for pure 5CB and a 0.809 wt % solution of TPB13 in 5CB. As evident in Figure 2b, it is clear that for this polymer solution, even at the smallest angle, 10° (lab frame), the difference between η_2 and γ_1 is around 5% due to the fact that the ratio of η_a to α_2^2 is very small. In principle, we can obtain K_{22}, K_{33}, γ_1, η_a/α_2^2, and η_c/α_2^2 by performing field-dependent light scattering measurements at different angles and generating numerical fits to eq 2a-2. However, since we can accurately measure decay rates only over a limited range 10–55°, the terms containing K_{33}, η_a/α_2^2, and η_c/α_2^2 do not contribute sufficiently to obtain reliable results. Therefore, we only determine γ_1 from field-dependent light scattering in the twist geometry. The twist viscosity of 5CB at ΔT = 7.5 °C obtained from Figure 2a agrees very well with the literature value reported by Skarp et al.[30]

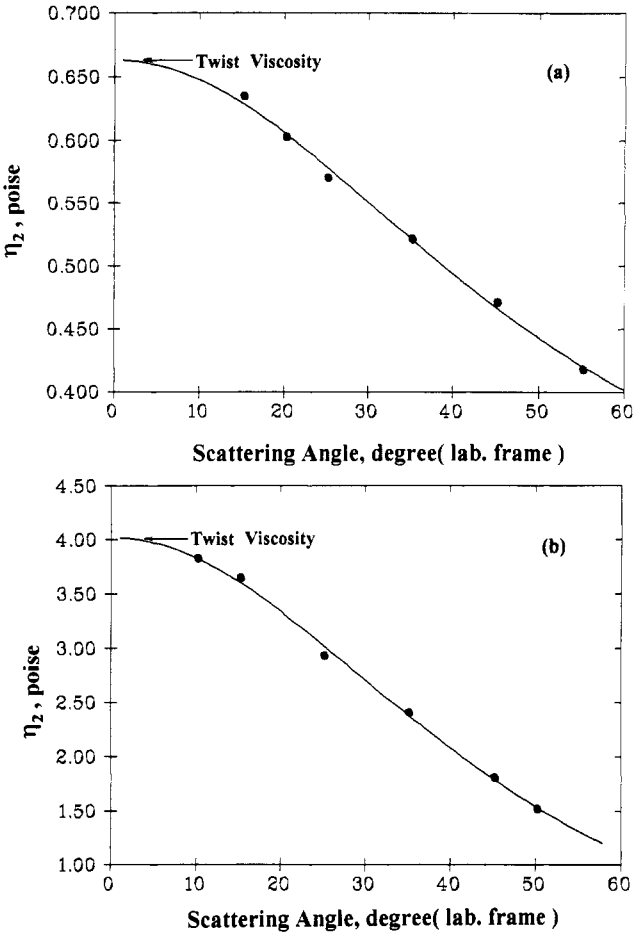

Figure 2. The dependence of the viscosity coefficient η_2 upon scattering angle in the lab frame: (a) pure 5CB and (b) 0.089 wt% TPB13 in 5CB at 27.3 °C. The solid lines are the best fits to eq 2a-2.

Table 2 lists the polymer concentrations of the various nematic solutions utilized in this investigation. These were selected to assure a conveniently measurable increment $\delta\gamma_1$ and yet remain within the linear regime for $\delta\gamma_1$ vs C. We have demonstrated previously[22] that linear additivity of the twist viscosity holds for TPB10 solutions in the concentration range $C[\gamma_1] \leq 12.1$. Here C is the polymer concentration in g/mL and the intrinsic twist viscosity $[\gamma_1] = \delta\gamma_1/(C\gamma_1°)$ where the viscosity increment $\delta\gamma_1 = \gamma_1 - \gamma_1°$, and γ_1 and $\gamma_1°$ are the twist viscosities of solutions and nematic solvent, respectively. In this study, as will be seen later, all the concentrations listed in Table 2 correspond to values of the product $C[\gamma_1]$ below 8. Thus, our measurements are well within the linear concentration regime where $[\gamma_1]$ is independent of polymer concentration.

Table 2. Experimental Concentrations of TPB10/5OCB, TPB10/5CB, TPB13/5OCB, and TPB13/5CB Solutions

solution	TPB10 dimer in 5OCB	TPB10 trimer in 5OCB	TPB10 tetramer in 5OCB	TPB10 no. 5 in 5OCB
concn wt%	9.99	6.71	5.01	1.564
solution	TPB10 no. 6 in 5OCB	TPB10 no. 7 in 5OCB	TPB no. 8 in 5OCB	TPB10 no. 9 in 5OCB
concn wt%	1.558	1.344	0.991	0.920
solution	TPB10 dimer in 5CB	TPB10 trimer in 5CB	TPB10 tetramer in 5CB	TPB13 in 5OCB
concn wt%	4.71	4.22	1.987	1.00
solution	TPB13 in 5 CB			
concn wt	0.809			

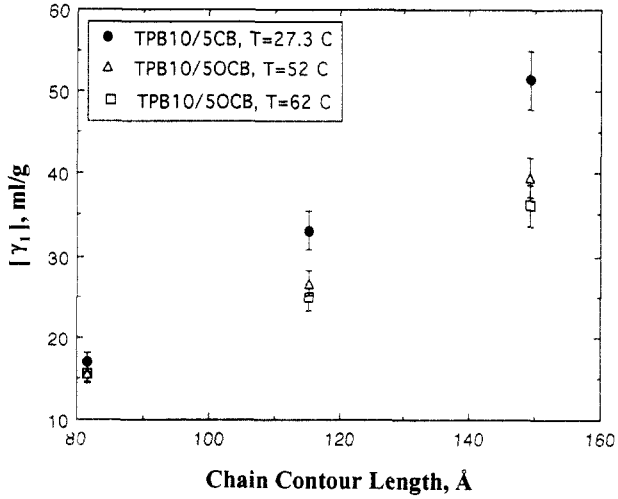

Figure 3. The dependence of the twist viscosity increment on chain contour length of TPB10 oligomers (dimer, trimer, and tetramer) in 5CB and 5OCB.

The dependence of the intrinsic twist viscosity on the chain contour length for TPB10 oligomers in 5OCB at ΔT = 5 (i.e. T = 62 °C) and 15 °C (i.e. T = 52 °C) and in 5CB at ΔT = 7.5 °C (i.e. T = 27.3 °C) are shown in Figure 3. To convert concentration in wt% to g/mL, the density of solutions was assumed to be that of the pure nematic solvent and was taken from existing data.[31] These temperatures were selected, first, because in 5OCB we compare the behavior of oligomers under conditions differing in both temperature and nematic potential; second, in 5CB at T = 27.3 °C and 5OCB at T = 62 °C, we contrast their behavior under conditions of comparable nematic order parameter[32,33] but with a large difference in absolute temperature (300.3 °K in 5CB vs 335 °K in 5OCB). Here we assume that the order parameter of solution is the same as that of the nematic solvent. In support of this we note that the difference in dielectric anisotropy ($\Delta\epsilon$) between these dilute solutions and the pure nematic solvent is very small (≤3%) (see Table 3). $\Delta\epsilon$ is proportional to the nematic order parameter provided the solution has the same molecular dipole moment and polarizability anisotropy as the pure solvent.[34] The nematic order parameters (S) of 5CB and 5OCB are also listed in Table 3.

From Figure 3, we see that TPB10 oligomers in 5CB at T = 27.3 °C have higher intrinsic twist viscosities than in 5OCB at T = 62 °C. Since these two solutions have a comparable order parameter, this indicates that the absolute temperature has a very strong influence on the intrinsic viscosity and hence on the molecular chain statistics. Also, in Figure 3, the dependence of the intrinsic twist viscosity on oligomer molecular weight is larger for TPB10/5CB (T = 27.3 °C) than for TPB10/5OCB (T = 62 °C). We interpret this result to indicate that decrease of temperature produces a substantial increase in chain extension of the tetramer, a smaller increase for the trimer, but does not significantly influence the dimer which is already essentially fully extended. In comparing TPB10/5OCB at T = 52 °C to TPB10/5OCB at T = 62 °C, we find a similar comparative trend. One important finding from Figure 3 is that $[\gamma_1]$ for TPB10 in 5CB at ΔT = 7.5 °C (i.e. T = 27.3 °C) is always larger than $[\gamma_1]$ for TPB10 in 5OCB at ΔT = 15 °C (i.e. T = 52 °C). Since the latter has approximately 20% higher nematic order parameter and only 8% higher temperature (in K) than the former, this is striking evidence that the temperature plays the dominant role over the order parameter in determining the degree of chain extension.

To further interpret these data, we now recall the theoretical prediction of Brochard[21]

$$\delta\gamma_1 = (CN_A/M)[\lambda_\parallel\lambda_\perp R_\parallel^2 R_\perp^2/(\lambda_\parallel R_\parallel^2 + \lambda_\perp R_\perp^2)] (R_\parallel^2 - R_\perp^2)^2/(R_\parallel^2 R_\perp^2) \quad (6)$$

where C is the polymer concentration in g/mL; N_A is the Avogadro's number; M is the molecular weight of the polymer; $\lambda_\parallel$ and $\lambda_\perp$ are, respectively, the friction coefficients associated with motions parallel and perpendicular to the director; and $R_\parallel^2$ and $R_\perp^2$ are the mean square end-to-end distances parallel and perpendicular to the director, respectively. We assume that eq 6 can be applied to oligomers as well as polymers. For the former, as pointed out by Brochard,[21] it is likely that a free-draining condition holds. Further, we anticipate that, hydrodynamically, the oligomers will behave like thin rods, for which Brochard[21] deduced $\delta\gamma_1 = (CN_A/M)\lambda_\perp R_\parallel^2$ (stick limit, $R_\parallel^2 \gg R_\perp^2$).

Assuming a free draining condition, i.e. $\lambda_\perp \propto M$, and $R_\parallel^2 \gg R_\perp^2$ are valid for the oligomers, it follows that[22]

$$[\gamma_1] \propto R_\parallel^2 \quad (7)$$

For a rigid rod, $R_\parallel \propto L$,[35] and

$$[\gamma_1] \propto L^2 \quad (8a)$$

Note that the contour length of the monomer (n = 1 in Figure 1, L = 47.7 Å) is much larger than that of the solvent 5CB (L = 17.3 Å). Also, we measured $[\gamma_1]$ for the monomer and found it to be positive. Nevertheless, we have not used the monomer result since the comparatively concentrated solution utilized shows a relatively large decrease in T_{NI} (≈−3 °C) implying a large change in order parameter.

Finally, we point out that, for the TPB10 polymers, we expect a biased random coil, $R_\parallel \propto L^{0.5}$ and $R_\perp \propto L^{0.5}$,[35]

$$[\gamma_1] \propto L \quad (8b)$$

By least squares fit, the chain contour length dependence of the intrinsic twist viscosity of TPB10 oligomers are found to be, for TPB10/5OCB at T = 62 °C:

$$[\gamma_1] = 0.03458L^{1.39} \quad (9a)$$

for TPB10/5OCB at T = 52.0 °C:

$$[\gamma_1] = 0.01832L^{1.53} \quad (9b)$$

Table 3. Dielectric Anisotropies of TPB10 Oligomer Solutions in 5CB and 5OCB

specimen	5OCB	TPB10 dimer in 5OCB	TPB10 trimer in 5OCB	TPB10 tetramer in 5OCB
$\Delta\epsilon \pm 3\%$, $\Delta T = 5$ °C	9.66	9.84	9.91	9.97
$\Delta T = 15$ °C	12.34	12.18	12.27	12.33
specimen	5CB	TPB10 dimer in 5CB	TPB10 trimer in 5CB	TPB10 tetramer in 5CB
$\Delta\epsilon \pm 3$, $\Delta T = 7.5$ °C	12.48	12.11	12.25	12.57
specimen		5CB ($\Delta T = 7.5$ °C)	5OCB ($\Delta T = 5$ °C)	5OCB ($\Delta T = 15$ °C)
order parameter		0.44[33]	0.44[32]	0.54[32]

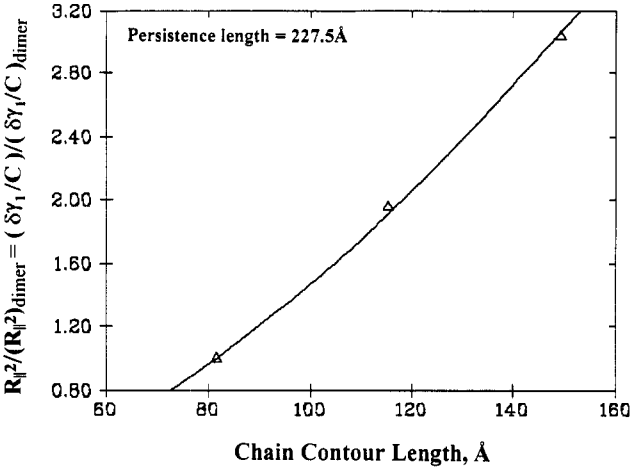

Figure 4. The dependence upon chain contour length of $R_\parallel^2/(R_\parallel^2)_{dimer}$ for TPB10 oligomers in 5CB at 27.3 °C. The solid line is the best fit to eq 10 and yields the persistence length $a = 227.5$ Å.

and, for TPB10/5CB at $T = 27.3$ °C:

$$[\gamma_1] = 0.00523L^{1.84} \tag{9c}$$

Note that eq 9b is slightly different from the previous result[22] resulting from improved precision in the determination of dielectric permittivity. Since we expect that the molecular extension along the director will increase with increasing nematic potential or decreasing temperature, the experimental results are therefore very consistent with eq 8a and indicate a closer approach to rigid rod behavior as temperature decreases. From eqs 9b and 9c, we note that the contour length exponent for TPB10 in 5CB at $T = 27.3$ °C is substantially larger than for TPB10 in 5OCB at $T = 52.0$ °C. This again shows that the absolute temperature has a much stronger effect than the nematic order parameter on the chain extension.

As we have shown previously,[22] we can obtain a quantitative estimate of the degree of chain extension by applying molecular models to interpret the intrinsic twist viscosity data of the oligomers. For example, utilizing the wormlike model, we derive[22]

$$\frac{R_\parallel^2}{(R_\parallel^2)_r} = \frac{L - a[1 - \exp(-L/a)]}{L_r - a[1 - \exp(-L_r/a)]} \tag{10}$$

where the subscript "r" refers to the reference species, i.e. the dimer, and a is the persistence length. From the Brochard model[21] via eq 7, we may further write:

$$\frac{\delta\gamma_1/C}{(\delta\gamma_1/C)_{dimer}} = \frac{R_\parallel^2}{(R_\parallel^2)_{dimer}} \tag{11}$$

Figure 4 shows the result of fitting the $\delta\gamma_1/C$ data for TPB10 oligomers in 5CB at $T = 27.3$ °C to eqs 10 and 11. The persistence lengths obtained in this way are listed in Table 4. Note that the value shown for TPB10/5OCB at 52 °C in Table 4 is significantly larger than that quoted in our earlier study.[22] This discrepancy occurs because, in our earlier interpretation of the Brochard theory, we mistakenly assumed the pertinent polymer size parameter in eq 11 to be the radius of gyration. Proper application of eq 11 leads to larger and intuitively more reasonable values for the persistence length, in view of the fact that the length of a fully-extended TPB10 repeat unit is 33.87 Å. Thus, from Table 4, the persistence length at the highest temperature is comparable to the repeat unit length.

Table 4. Persistence Lengths, Hairpin Turn Probabilities, and Exponents α in $[\eta] \propto L^\alpha$ for $[\gamma_1]$ and $[\eta_{bend}]$ of TPB10 Oligomers in 5CB and 5OCB

	mixture		
	TPB10 oligomers in 5CB	TPB10 oligomers in 5OCB	
T, °C	27.3	52.0	62.0
$[\eta_{bend}] \propto L^\alpha$	$\alpha = 1.11$	$\alpha = 0.67$	$\alpha = 0.46$
$[\gamma_1] \propto L^\beta$	$\beta = 1.84$	$\beta = 1.53$	$\beta = 1.39$
persistence length	227.5 Å	55.4 Å	34.3 Å
hairpin turn probability	0.09 ± 0.03	0.22 ± 0.05	0.27 ± 0.07

Alternatively, we can attempt a more microscopic analysis of the configurational states present in the oligomer solutions. To achieve this, as before,[22] we model the oligomer solutions as mixtures of configurational isomers containing either no hairpins or a single hairpin. Assuming eq 8 is applicable to all configurational isomers, i.e. $[\gamma_1] \propto L_i^2$, and realizing that $[\gamma_1] = \sum W_i[\gamma_1]_i$, we have[22]

$$[\gamma_1]_{dimer} \propto (1 - P)81.5^2 + P40.75^2 \tag{12a}$$

$$[\gamma_1]_{trimer} \propto (1 - 2P)115.4^2 + 2P74.65^2 \tag{12b}$$

$$[\gamma_1]_{tetramer} \propto [1 - 3P)149.3^2 + 2P108.55^2 + P74.65^2 \tag{12c}$$

where P is the probability of a hairpin per repeat unit. Note that the contour length of each species includes a contribution from the extra decamethylene tail (Figure 1) in addition to the length of the repeat unit. Utilizing the experimental values of $[\gamma_1]$ for dimer, trimer and tetramer, we can now determine the value of P from the experimental ratios $[\gamma_1]_{dimer}/[\gamma_1]_{trimer}$, $[\gamma_1]_{dimer}/[\gamma_1]_{tetramer}$, and $[\gamma_1]_{trimer}/[\gamma_1]_{tetramer}$ for each temperature. The results are listed in Table 4. Since we expect that P and a are determined by changes in population of trans and gauche conformational states, it follows that each should exhibit Arrhenius relationship with temperature. The activation energy to the hairpin probability and persistence length can be determined, respectively, via $P \propto \exp(-E_P/_RT)$ and $a \propto \exp(Ea/RT)$. In this calculation, we also include the data from TPB10 oligomers in 5OCB at $T = 52$ °C despite the fact that these systems have a larger nematic order parameter than the others, since we have shown that the absolute temperature is the dominant factor. The activation energies for persistence length and hairpin probability obtained in this way are:

$$E_p = 6.4 \text{ kcal/mol} \tag{13a}$$

$$E_a = 10.9 \text{ kcal/mol} \tag{13b}$$

where the subscript "P" refers to hairpin probability and "a" refers to persistence length. Since formation of a hairpin turn requires two gauche conformations (g+ and g−), and since the energy barrier for a trans to gauche

Table 5. Bend Diffusivity Ratios of 5OCB, 5CB, TPB13/5CB, and TPB13/5OCB

specimen	5OCB	TPB10 dimer in 5OCB	TPB10 trimer in 5OCB	TPB10 tetramer in 5OCB
$(K_{33}/\eta_{bend}) \pm 2\%$, $\Delta T = 5$ °C	705.3	514.4	550.3	565.5
$(10^{-8}$ cm^2/s) $\Delta T = 15$ °C	725.9	521.0	548.3	559.5

specimen	TPB10 no. 5 in 5OCB	TPB10 no. 6 in 5OCB	TPB10 no. 7 in 5OCB	TPB10 no. 8 in 5OCB	TPB10 no. 9 in 5OCB
$(K_{33}/\eta_{bend}) \pm 2$, $\Delta T = 5$ °C	576.2	558.7	567.8	565.4	553.2
$(10^{-8}$ cm^2/s) $\Delta T = 15$ °C	557.5	547.0	549.8	566.4	560.3

specimen	5CB	TPB10 dimer in 5CB	TPB10 trimer in 5CB	TPB10 tetramer in 5CB
$(K_{33}/\eta_{bend}) \pm 2\%$, $\Delta T = 5$ °C $(10^{-8}$ cm^2/s)	543.1	463.4	443.0	475.5

transformation is about 3.4 kcal/mol,[36] it appears that the activation energy values deduced are of the right order of magnitude.

b. Bend Viscosity of TPB10 Oligomers and Polymers. To investigate the temperature- and the molecular weight-dependence of the bend distortion, we compared the bend decay rates for TPB10/5CB mixtures and pure 5CB at $\Delta T = 7.5$ °C, and for TPB10/5OCB mixtures and pure 5OCB at $\Delta T = 5.0$ °C and 15 °C. Values for the bend diffusivity ratio K_{33}/η_{bend} calculated via eq 3 at $q_\perp = 0$ are presented in Table 5. Since the polymer concentrations in these solutions, listed in Table 2, are not identical, to compare the effectiveness of the addition of polymer in decreasing the decay rates, we define the intrinsic inverse decay rate as

$$[\bar{\Gamma}^{-1}_{bend}] = \frac{\bar{\Gamma}_{bend,o} - \bar{\Gamma}_{bend}}{C\bar{\Gamma}_{bend}} = \frac{\left(\frac{K_{33}}{\eta_{bend}}\right)_o - \frac{K_{33}}{\eta_{bend}}}{C\frac{K_{33}}{\eta_{bend}}} \quad (14)$$

where C is the polymer concentration in g/mL and the subscript "o" refers to pure nematic solvent. From eq 14, we note that if $K_{33} = (K_{33})_o$, then

$$[\bar{\Gamma}^{-1}_{bend}] = [\eta_{bend}] = \frac{\eta_{bend} - \eta_{bend,o}}{C\eta_{bend,o}} \quad (15)$$

In principle, we can obtain the bend viscosity by measuring light scattering decay rates in the twist and bend geometries and generating simultaneous fits to eqs 2 and 3. However, the uncertainty for bend viscosity determined in this way is up to 10% resulting in a 60% uncertainty for intrinsic bend viscosity. Since our earlier work[3] indicates that the change in decay rates on addition of polymer is primarily determined by the change of the viscosity, we assume for the sake of discussion that $[\Gamma_{bend}{}^{-1}]$ is numerically equal to $[\eta_{bend}]$.

In Figure 5, we compare the molecular weight dependence of $[\gamma_1]$ and $[\eta_{bend}]$ for TPB10/5OCB at $\Delta T = 15$ °C. As evident in Figure 5 for the oligomer mixtures whose viscous behavior is dominated by fully-extended chains which behave like rigid rods, $[\eta_{bend}]$ is a strongly-increasing function of chain contour length. In contrast, for the polymers, which we have interpreted as behaving like a free-draining random coil,[22] $[\eta_{bend}]$ shows only a very weak dependence on contour length. Thus, if the polymer molecular weight is large enough, $[\eta_{bend}]$ is essentially constant within the experimental error, which is consistent with our previous observations[10,14,15] on nematic solutions of TPBx polymers of different spacer lengths. It is interesting to contrast our observations in Figure 5 with those of Lee and Meyer[37] who determined γ_1 and η_{bend} for lyotropic nematic solutions of poly-γ-benzyl glutamate (PBG) in dioxane/dichloromethane (18/82). These authors found that η_{bend} increased with molecular weight for polymers whose chain lengths (L) are shorter than the persistence length (a) and was essentially constant for polymers with $L > a$. On the other hand, the twist viscosity

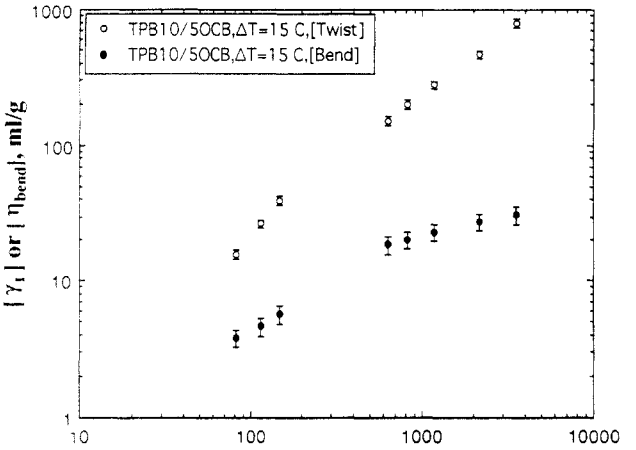

Figure 5. The dependence of $[\gamma_1]$ and $[\eta_{bend}]$ upon the weight average chain contour length of TPB10 in 5OCB at $\Delta T = 15$ °C.

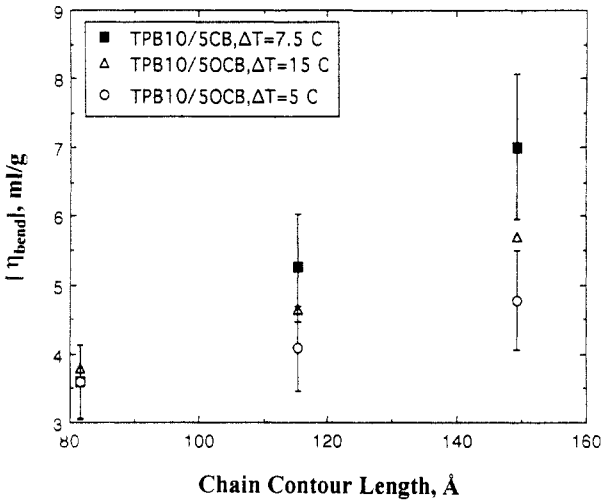

Figure 6. The dependence of $[\eta_{bend}]$ on the chain contour length of TPB10 oligomers in 5CB and 5OCB.

increased strongly with chain length for all polymers, and no change in the dependence of twist viscosity on chain length was observed at $L \approx a$. Experimentally, we find $[\eta_{bend}] \propto L^{0.67}$ for the oligomers and $[\eta_{bend}] \propto L_w{}^{0.30}$ for the polymers. Physically, this result seems reasonable. As noted by Lee and Meyer,[37] motions which involve bending of the molecular axis are expected to become less sensitive to chain length when the chain length exceeds the persistence length.

We have examined the temperature dependence of $[\eta_{bend}]$ for TPB10 oligomers and polymers in 5OCB at $\Delta T = 5$ °C and 15 °C. We find that $[\eta_{bend}]$ at the lower temperature is slightly larger, however, the difference is rather small and close to experimental error. In Figure 6, we compare $[\eta_{bend}]$ of the TPB10 oligomers in 5OCB at $\Delta T = 5$ °C and 15 °C with that in 5CB at $\Delta T = 7.5$ °C. The results parallel those observed for $[\gamma_1]$, i.e. the small differences between $[\eta_{bend}]$ at lower and higher tempera-

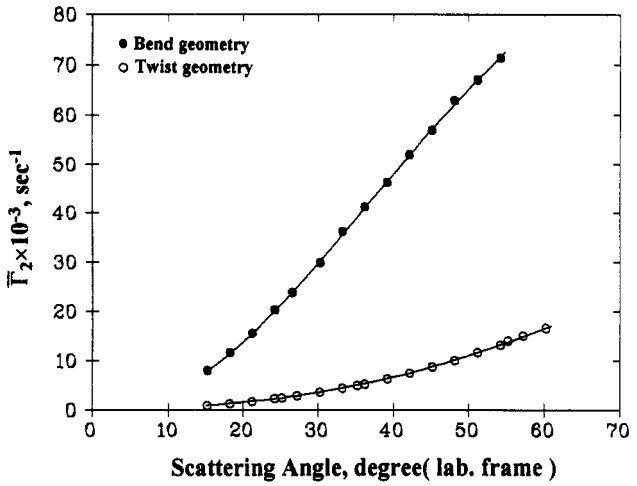

Figure 7. The dependence of average decay rate upon the scattering angle in the lab frame for pure 5CB at ΔT = 7.5 °C.

Table 6. Viscometric Properties of 5CB, 5OCB, TPB13/5CB, and TPB13/5OCB

	specimen			
	5CB	TPB13/5CB (0.809 wt%)	5OCB	TPB13/5OCB (1.00 wt%)
T, °C	27.3	27.3	62.0	62.0
order parameter	0.44	0.44[a]	0.44	0.44[a]
$\gamma_1 \pm 4\%$, poise	0.664	4.03	0.262	1.34
$\eta_{splay} \pm 7\%$, poise	0.655	3.64	0.259	1.14
$\eta_{bend} \pm 10\%$, poise	0.133	0.181	0.061	0.085
$\eta_c \pm 15\%$, poise	0.934	4.89	0.385	1.80
$\eta_b \pm 20\%$, poise	0.190	0.244	0.0914	0.134
$\eta_a \pm 20\%$, poise	0.283	0.396	0.153	0.237

[a] Order parameter of pure nematic solvent.

tures increase with molecular weight. Also, the effect of temperature is stronger than that of the order parameter. The exponents α in the relationship $[\eta_{bend}] \propto L^{\alpha}$ are listed in Table 4 which also includes the exponents in $[\gamma_1] \propto L^{\beta}$ for comparison. From Table 4, we find that as the exponent β shifts toward the rigid rod value β = 2.0, the exponent α appears to be tending toward a value near unity.

c. Temperature Dependence of Anisotropic Viscosities of TPB13 Polymer. In the following, we wish to focus our attention on the effect of absolute temperature on the viscometric properties of TPBx polymers in nematic solvents. In order to obtain all of the anisotropic viscosities, we performed all of the experiments cited in the Experimental Section. We obtained independently γ_1 by electric field-dependent light scattering in the twist geometry and then performed a four parameter simultaneous curve fitting analysis to the data in scattering configurations II and II via eqs 2a-1 and 3. The corresponding dependence of average decay rates on the scattering angle in the lab frame for pure 5CB at ΔT = 7.5 °C and the best fits to eqs 2a-1 and 3 are shown in Figure 7. The nonlinear curve fitting program we used is MINSQ (Micromath, Salt Lake, UT). From this analysis we obtain K_{22}, K_{33}, η_a/α^2, and η_c/α^2. From the Freedericksz transition measurements we have K_{11} and from light scattering measurements of the pure splay mode we have K_{11}/η_{splay}. Utilizing the relationships, $\alpha_3 = \gamma_1 + \alpha_2$ and $\eta_b = \eta_c + \alpha_3 + \alpha_2$, together with the definition of the splay viscosity (eq 1c), we are able to determine all the individual viscosities. In Table 6, we list various viscosities for pure 5OCB and TPB13/5OCB at T = 62 °C (ΔT = 5 °C), and for pure 5CB and TPB13/5CB at T = 27.3 °C (ΔT = 7.5 °C). From these results, we are able to calculate the intrinsic viscosities as shown in Table 7. In this table, we first note that $[\eta_{bend}]$ $\approx [\eta_b]$ as expected. Second, we see that TPB13 in 5CB at ΔT = 7.5 °C has a substantially larger $[\gamma_1]$, $[\eta_{splay}]$, and $[\eta_c]$ than in 5OCB at ΔT = 5 °C; however, in each system $[\eta_{bend}]$, $[\eta_a]$, and $[\eta_b]$ are numerically similar. Since 5CB at ΔT = 7.5 °C and 5OCB at ΔT = 5 °C have identical nematic order parameters, it is clear that the absolute temperature has a large influence on $[\gamma_1]$, $[\eta_{splay}]$, and $[\eta_c]$. There appears to be little effect of temperature on $[\eta_{bend}]$, $[\eta_a]$, and $[\eta_b]$, but we note the relatively large errors in these small increments.

Table 7. Intrinsic Viscosities and Configurational Chain Anisotropies of TPB13/5CB and TPB13/5OCB

	solution	
	TPB13/5CB	TPB13/5OCB
T, °C	27.3	62.0
order parameter	0.44[a]	0.44[a]
$[\gamma_1]$(mL/g) ± 8%	615	399
$[\eta_{splay}]$(mL/g) ± 15%	553	330
$[\eta_{bend}]$(mL/g) ± 60%	44	37
$[\eta_c]$(mL/g) ± 30%	514	356
$[\eta_b]$(mL/g) ± 70%	35	45
$[\eta_a]$(mL/g) ± 70%	48	53
$(R_\parallel/R_\perp)$ ± 50%	3.6	2.8

[a] Order parameter of pure nematic solvent.

In the preceding discussion, we have shown that eq 6 can be applied to rationalize the experimental behavior of γ_1, and since η_c and γ_1 are each dominated by rotational motion of the director, we assume that the following equation from Brochard model[21] will also be useful

$$\delta\eta_c = \frac{CN_A}{M} \frac{\lambda_\parallel \lambda_\perp R_\perp^{\,2}}{\lambda_\parallel R_\parallel^{\,2} + \lambda_\perp R_\perp^{\,2}} \tag{16}$$

From eqs 6 and 16, we may write

$$\left(\frac{\delta\gamma_1}{\delta\eta_c}\right)^{1/2} = 1 - \frac{R_\perp^{\,2}}{R_\parallel^{\,2}} \tag{17}$$

Inserting experimental values of η_c and γ_1 for pure nematic solvent and mixture, eq 17 yields estimates of $R_\parallel/R_\perp$ which are listed in Table 7. As expected, the chain configuration of TPB13 in 5CB at ΔT = 7.5 °C and in 5OCB at ΔT = 5 °C is prolate, i.e. $R_\parallel > R_\perp$, and we find that the chain anisotropy $(R_\parallel/R_\perp)$ for TPB13 in 5CB at ΔT = 7.5 °C is 28% larger than in 5OCB at ΔT = 5 °C. Thus the increased values of $[\gamma_1]$, $[\eta_{splay}]$, and $[\eta_c]$ at lower temperature can be interpreted as due to a larger $R_\parallel$ resulting from a larger persistence length or smaller hairpin probability.

Finally, we comment on the absolute values of the intrinsic viscosities listed in Table 7. From the weight-average molecular weight of the TPB13 sample, measured by GPC using polystyrene standards in chloroform, we can estimate, using published viscosity–molecular weight relationships[39] for polystyrene in good solvents, that the hydrodynamic volume in the isotropic state is $V_h \approx 2100$ nm^3 corresponding to a hydrodynamic radius $R_h \approx 8$ nm. To calculate the intrinsic viscosity of TPB13 in the isotropic state, we must know the actual molecular weight (M). We used the correction, $M = M_{GPC}/1.6$, for TPB10.[23] Thus the intrinsic viscosity is found to be $[\eta] \approx 64$ mL/g. From Table 7, we can compare this with the Miesowicz simple shear intrinsic viscosities in the nematic state at 27.3 °C: $[\eta_c]$ = 514 mL/g, R_h = 15.9 nm, where the director is aligned in the shear plane perpendicular to the flow direction; $[\eta_b]$ = 35 mL/g, R_h = 6.5 nm, where the director is in the shear plane parallel to the flow direction; and $[\eta_a]$ = 48 mL/g, R_h = 7.2 nm, where the director is along the vorticity axis. Thus, our observations lead to the intu-

itively reasonable result that the effective hydrodynamic radius in the nematic state, when the major chain axis is oriented parallel to the flow or along the vorticity axis, is slightly smaller to that in the isotropic state, but is substantially larger when the chain axis is perpendicular to the flow direction and the vorticity axis.

Conclusions

We have investigated the molecular weight dependence of the intrinsic twist viscosity and bend viscosity of a main chain LCP, TPBx with x = 10 and 13, in 5OCB and 5CB at different temperatures. We find that the influence of absolute temperature is much stronger than that of the nematic order parameter on the magnitude of the intrinsic twist viscosity and hence on the configurational anisotropy of the chains. The behavior of the twist viscosities of TPB10 oligomers suggests that the hydrodynamic behavior tends toward that of a rigid rod as the temperature decreases. The expression for $\delta\gamma_1$ from the Brochard model can be used to interpret the experimental observations. The persistence length obtained through analysis of the oligomer data in terms of the wormlike chain is found to increase with decreasing temperature. By modeling the oligomer solutions as mixtures of configurational isomers containing either no hairpins or one hairpin, the hairpin probability per repeat unit can be estimated and is found to decrease with decreasing temperature. The activation energies for persistence length and hairpin probability are, respectively, 10.9 and 6.4 kcal/mol, which are, respectively, $\sim\times3$ and $\sim\times2$ the energy barrier for a trans to gauche transformation, two of which are required for formation of a hairpin turn.

The molecular weight dependence of the intrinsic bend viscosity is weak relative to that of the intrinsic twist viscosity. In both $[\gamma_1]$ and $[\eta_{bend}]$, a crossover from stronger molecular weight dependence for the oligomers to weaker for the polymers is observed, which appears to correspond to the transition from a nearly rigid rod to a biased random coil.

Finally, we investigated the effect of temperature upon the viscometric properties of TPB13 in 5CB at T = 27.3 °C and in 5OCB at T = 62 °C where the nematic order parameters are essentially identical $S \sim 0.44$. We find that TPB13/5CB at T = 27.3 °C has substantially higher $[\gamma_1]$, $[\eta_{splay}]$, and $[\eta_c]$ than TPB13/5OCB at T = 62 °C. However, $[\eta_{bend}]$, $[\eta_a]$, and $[\eta_b]$ are numerically similar in each system. This result can be attributed to a larger chain extension along the director, i.e. an increase in $R_\parallel$ at lower temperature. Numerically reasonable values are computed for the ratio of the end-to-end distances, $R_\parallel/R_\perp$, and for the effective hydrodynamic radii.

Acknowledgment. We would like to thank Prof. Virgil Percec at Case Western Reserve University for kindly supplying the main-chain LCP. Also, we thank Mr. Pat Dunn at Kent State University for the courtesy of polyimide-coated glass slide. Finally, financial support from NSF Materials Research Group DMR 08145 is gratefully acknowledged.

References and Notes

(1) Mattoussi, H.; Ober, R. *Macromolecules* **1990**, *23*, 1809.
(2) D'Allest, J. F.; Sixou, P.; Blumstein, A.; Blumstein, R. B.; Teixeira, J.; Noirez, L. *Mol. Cryst. Liq. Cryst.* **1988**, *155*, 581.
(3) Gu, D.; Jamieson, A. M.; Rosenblatt, C.; Tomazos, D.; Lee, M.; Percec, V. *Macromolecules* **1991**, *24*, 2385.
(4) Weil, C.; Casagrande, C.; Veyssie, M. *J. Phys. (Paris)* **1986**, *47*, 887.
(5) Mattoussi, H.; Veyssie, M. *J. Phys. (Paris)* **1989**, *50*, 99.
(6) Mattoussi, H. *Mol. Cryst. Liq. Cryst.* **1990**, *178*, 65.
(7) Pashkovsky, E. E.; Litvina, T. G. *J. Phys. II (Paris)* **1992**, *2*, 521.
(8) Pashkovsky, E. E.; Litvina, T. G.; Kostromin, S. G.; Shibaev, V. P. *J. Phys. II (Paris)* **1992**, *2*, 1577.
(9) Pashkovskii, Ye. E.; Litvina, T. G. *Polym. Sci.* **1991**, *33*, 655.
(10) Gu, D.-F.; Jamieson, A. M.; Lee, M.-S.; Kawasumi, M.; Percec, V. *Liq. Cryst.* **1992**, *12*, 961.
(11) Gu, D.; Smith, S. R.; Jamieson, A. M.; Lee, M.; Percec, V. *J. Phys. II (Paris)* **1993**, *3*, 937.
(12) Gilli, J. M.; Sixou, P.; Blumstein, A. *J. Polym. Sci.: Polym. Lett. Ed.* **1985**, *23*, 379.
(13) Coles, H. J.; Sefton, M. S. *Mol. Cryst. Liq. Cryst. Lett.* **1985**, *1*, 159.
(14) Gu, D.; Jamieson, A. M.; Kawasumi, M.; Lee, M.; Percec, V. *Macromolecules* **1992**, *25*, 2152.
(15) Chen, F.-L.; Jamieson, A. M. *Macromolecules* **1993**, *26*, 6576.
(16) Brochard, F.; Pieranski, P.; Guyon, E. *J. Phys. (Paris)* **1972**, *33*, 681 and **1973**, *34*, 35.
(17) Brochard, F.; Pieranski, P.; Guyon, E. *Phys. Rev. Lett.* **1972**, *28*, 1681.
(18) Orsay Liquid Crystal Group. *J. Chem. Phys.* **1969**, *51*, 816.
(19) Orsay Liquid Crystal Group. *Phys. Rev. Lett.* **1969**, *22*, 1361.
(20) Sefton, M. S.; Bowdler, A. R.; Coles, H. J. *Mol. Cryst. Liq. Cryst.* **1985**, *129*, 1.
(21) Brochard, F. *J. Polym. Sci.: Polym. Phys. Ed.* **1979**, *17*, 1367.
(22) Chen, F.-L.; Jamieson, A. M. *Macromolecules* **1994**, *27*, 1943.
(23) Kawasumi, M. Ph.D. Thesis, 1993, Department of Macromolecular Science, Case Western Reserve University, Cleveland, OH, 44106.
(24) Chen, F.-L.; Jamieson, A. M. *Liq. Cryst.* **1993**, *15*, 171.
(25) Kinzer, D. *Mol. Cryst. Liq. Cryst. Lett.* **1985**, *1*, 147.
(26) Leslie, F. M. Q. *J. Mech. Appl. Math.* **1966**, *19*, 357.
(27) Miesowicz, M. *Bull. Int. Acad. Pol. Sci. Lett. Ser. A* **1936**, *28*, 228.
(28) Leslie, F. M.; Waters, C. M. *Mol. Cryst. Liq. Cryst.* **1985**, *123*, 101.
(29) Meyerhofer, D. *J. Appl. Phys.* **1975**, *46*, 5084.
(30) Skarp, K.; Lagerwall, S. T.; Stebler, B. *Mol. Cryst. Liq. Cryst.* **1980**, *60*, 215.
(31) Bradshaw, M. J.; Raynes, E. P.; Bunning, J. D.; Faber, T. E. *J. Phys. (Paris)* **1985**, *46*, 1513.
(32) Mitra, M.; Paul, R.; Paul, S. *Acta Physica Polonica* **1990**, *A78*, 453.
(33) Karat, P. P.; Madhusudana, N. V. *Mol. Cryst. Liq. Cryst.* **1976**, *36*, 51.
(34) de Jeu, W. H. *Physical Properties of Liquid Crystalline Materials*; Gordon and Breach: London, 1980.
(35) Warner, M.; Gunn, J. M. F.; Baumgärtner, A. B. *J. Phys. A; Math. Gen.* **1985**, *18*, 3007.
(36) Morrison, R. T.; Boyd, R. N. *Organic Chemistry*, 4th ed.; Allyn and Bacon: Boston, 1983, 85.
(37) Lee, S.-D.; Meyer, R. B. *Phys. Rev. Lett.* **1988**, *61*, 2217.
(38) Meyer, R. B. In *Polymer Liquid Crystals*; Ciferri, A., Krigbaum, W. R., Meyer, R. B., Eds.; Academic: New York, 1982; Chapter 6.
(39) Orofino, T. A.; Wenger, F. *J. Phys. Chem.* **1963**, *67*, 566.